Response of an REG-Driven Robot to Operator Intention

R.G. Jahn,* B.J. Dunne, D.J. Acunzo, and E.S. Hoeger

Princeton Engineering Anomalies Research Laboratory
School of Engineering and Applied Science
Princeton University, Princeton NJ 08544-5263

Abstract — A small articulating robot driven by an on-board miniaturized random event generator (REG) executes two-dimensional stochastic motion on a circular platform. Human operators attempt, under pre-recorded intentions, to influence the device to reach particular exit positions around the table edge, or to remain in motion on the table for longer, or shorter, time periods, or to cover longer, or shorter, overall distances than characterize a large body of unattended calibration data. An overhead camera system tracks the robot trajectories and transmits them to database storage for subsequent analysis. Each of several protocols yields overall results that clearly separate in the directions of operator intention, with effect sizes comparable to those found in many other REG-based experiments. Although the databases are not sufficiently large to drive all of these to statistical significance by the usual $p \leq .05$ criterion, certain operator subsets, most notably the females, the groups, and a few individuals, display more noteworthy performances. The consistency of this structural pattern of results with those obtained previously using substantially different equipment and protocols reinforces a generic character of such phenomena that eventually may lead to a useful comprehensive model for their representation and possible pragmatic applications.

Keywords: consciousness — humadmachine anomalies — robot — random event generator (REG)

1. Background and Introduction

As described in greater detail in a major review article,' a large portion of the PEAR experimental agenda has entailed a variety of human/machine interactions featuring feedback modalities designed to enhance emotional resonance between the operators and the target devices. These have included such diverse displays as a cascade of balls through a matrix of scattering pins, a large free-swinging pendulum, an upward bubbling water jet, competing visual images on a computer screen, and acoustical beats from a Native American drum, among others. For the particular experiment reviewed herein, a small mechanical robot driven by a miniaturized on-board REG was designed,

---

* Correspondence address: Mechanical and Aerospace Engineering, Engineering Quadrangle, Princeton University, Princeton NJ 08544

constructed, and deployed to execute two-dimensional stochastic motion on a circular table-top.

The concept for this experiment was stimulated by a succession of collegial interactions with a French scholar, René Péoc'h, who himself had appropriated robotic inventions of two colleagues, P. Janin[2] and R. Tanguy,[3] termed "tychoscopes," for experiments involving young chicks and rabbits.[4] From these studies, Péoc'h established the capacity of these animals to affect the trajectory of the robot to their biological advantages, by some anomalous means.[5]

Our extension of these techniques to experiments with human operators has addressed the hypothesis that an anthropomorphic resonance with the behavior of such a robot would enhance anomalous alterations of its random trajectory, with corresponding departures of the digital output of the REG unit directing it. The on-board mechanism driving the device has evolved empirically over the course of these experiments to correct various operational difficulties, such as wheel slippage, battery drain, initial alignment, etc., eventually reaching the form detailed in the Appendix. Briefly, it comprises two independent, battery-powered clock motors, each controlling one wheel of the robot. These in turn are instructed by the REG unit to drive the wheels by a sequence of various incremental amounts, thereby accomplishing a random array of forward translations and clockwise or counter-clockwise rotations of the vehicle on a 48-inch-diameter circular platform. From a set initial position and direction at the center of the table, the device executes a two-dimensional stochastic trajectory, eventually reaching the table: edge. The equipment is deployed in one of our principal experimental rooms, with the operators seated adjacent to the table, but having no contact with it (Figure 1). To enhance its whimsical attractiveness for the experimental operators, the electrical and mechanical components of the robot are encased in a 15-cm dome-shaped housing somewhat resembling a miniature Zamboni machine, with a toy frog perched in a driving position (Figure 2).
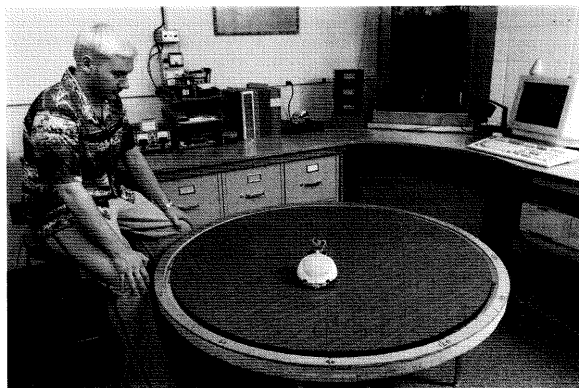

Fig. 1. PEAR Robot on its operating platform in a multi-purpose experimental room.
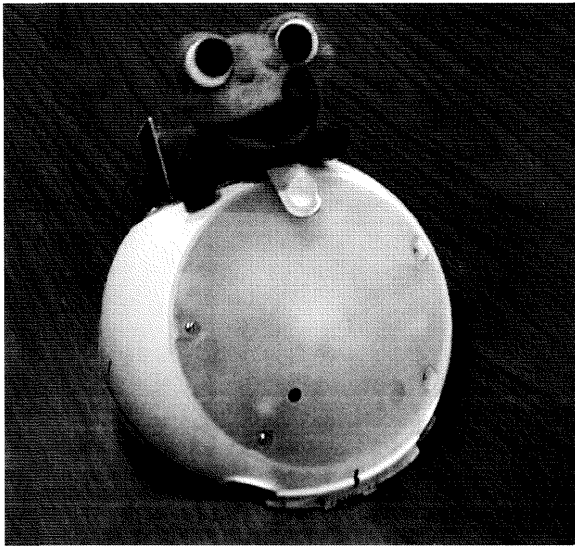
Fig 2 Close-up of PEAR Robot.

Before committing many operators to accumulation of the large datasets that are a sine *qua non* of any such human/machine/anomalies experiments, a few rudimentary pilot studies were performed by a limited number of operators attempting to bias the distribution of the exit angles of the robot at the table edge. These yielded some substantially larger anomalous effect sizes than those typically seen in our benchmark REG experiment,[6] encouraging further refinement of the equipment and the subsequent collection of the requisite large databases, as detailed in the following sections. Most notably, a small LED was added to the robot dome, which could be tracked by an overhead digital caniera, which in turn transmitted real-time specification of the entire course of the robot trajectory to a dedicated computer and database manager. This allowed each experimental run to be stored numerically and graphically for subsequent analyses (Figure 3).

2. Exit-Angle Experiments

In the first version of the formal experiments, the alternating intentions of the operators are simply to induce the robot to wander from its initial placement at the center of the table to exit locations as near as possible to the operator's initial position (denoted 0°), or directly opposite (180°). Each such effort is termed a "run," and two successive alternative efforts, a "set." Three phases of data collection, distinguished by minor adjustments to the robot, table, camera
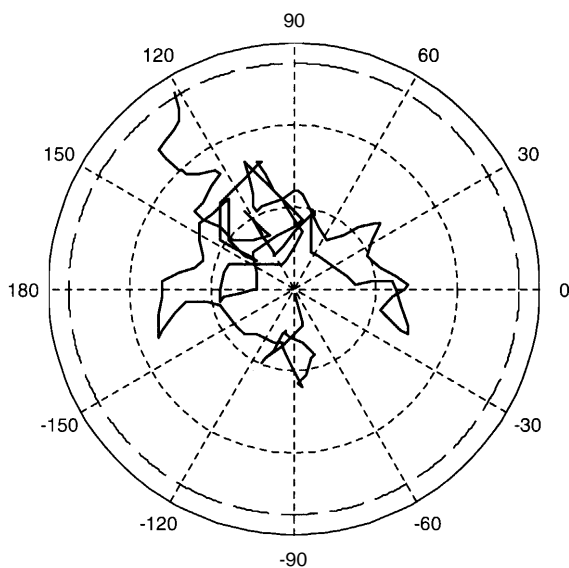
Fig. **3.** Print-out of digitized robot trajectory extracted from overhead camera datafile.

alignment, and operator positioning[†] have been conducted, each accompanied by its own calibration set. For this article, all of these formal data have been combined into one composite database, which is summarized in Table 1 and fully detailed in an associated Technical Report.[7] The participating operators have been divided into females, males, dual co-operators, and larger groups. Of the ten co-operator pairs, three were female/female, none male/male, and seven female/male. The six groups comprised from three to fifteen participants, and in three cases were children, in three cases young adults.

From the table it appears that even though the all-operator database is statistically unimpressive by a Z-score, effect size, or χ^2 criterion, the female sub-group achieves a modestly significant separation of the 0"-intention efforts from the 180"-intention efforts, with an equivalent effect size nearly three times larger than the all-operator data. The group performance displays an even more substantial effect size, which attains marginal significance even for this relatively small number of experimental sets. Both of these subsets also exceed

---

[†] In most cases, operators located themselves at the 0" table position for the 0" efforts, and moved to the 180" position for the 180" efforts. Thus, both entailed efforts to *attract* the robot toward themselves. In a few cases, operators remained at the 0" position for both attempts, hence the 180° data followed from efforts to repel the robot. Insufficient data have been acquired in this latter protocol variant to allow meaningful statistical comparisons. Hence, the primary differential data discriminator is the exit-angle target intention, rather than the attract/repel nuance.

TABLE 1
Summary of All Exit-angle Experiments 0° vs. 180°

Oper	# Ops	# Sets	$Z(p_z)$	ε	$\chi^2_{op}(p_\chi)$	# Oper +
All	87	1120	.957(.169)	.0286	85.561(.524)	48
Female	41	567	1.878(.030)*	.0789	50.743(.142)	27*
Male	30	416	−1.164(.880)	−.0571	23.011(.815)	12
Co-Operator	10	72	−.298(.617)	−.0351	5.444(.860)	4
Groups	6	67	1.738(.041)*	.2123	6.363(.384)	5*
Calibration	—	348	.810(.209)	.0434	—	—

Key

# Ops:	Number of individual operators, operator pairs, or groups contributing to the databases.
# Sets:	Number of 0°, 180° paired sets performed.
Z:	Statistical Z-scores computed from T-scores via Rosenthal approximation (*cf.* Appendix B of reference 7).
p_z:	One-tailed probabilities of Z-scores against chance expectations (* denotes significance at $p_z \leq .050$).
ε:	Equivalent effect size, computed as $Z/\sqrt{\#\text{Sets}}$.
χ^2_{op}:	Statistical chi-squared calculations over individual operator Z-scores; *i.e.*, $\sum_{ops} Z^2$ to be compared with the number of degrees of freedom (number of operators) to estimate the structural probabilities of the Z distributions compared to chance expectations.
p_χ:	chance probabilities of χ^2 values.
# Oper +:	Number of operators exceeding chance mean expectations in the intended directions.

chance by the criterion of the fractions of operators showing separations in the intended directions, *i.e.,* having collective positive Z-scores.

Quantitative comparison of these effect sizes with other REG-based experiments is inescapably somewhat arbitrary, given the disparities in the manners in which the basic binary samples are operationally deployed. However, if we refer to our extensive "benchmark" database,' with its more than 1.6 million, 200-sample differential (high − low) trials, and argue that performance of 200-trial "runs" thereof involve comparable operator time and effort to the robot sets, their comparison effect size figure is approximately $\varepsilon = .04$, *i.e.* very much in the same range as the robot data.

The effect sizes can provide a more commensurate indication of the statistical distinguishability of the various robot data subsets, via the basic relation for difference Z-scores:

$$Z_{i,j} = (\varepsilon_i - \varepsilon_j)/\sqrt{1/N_i + 1/N_j}$$

or equivalently:

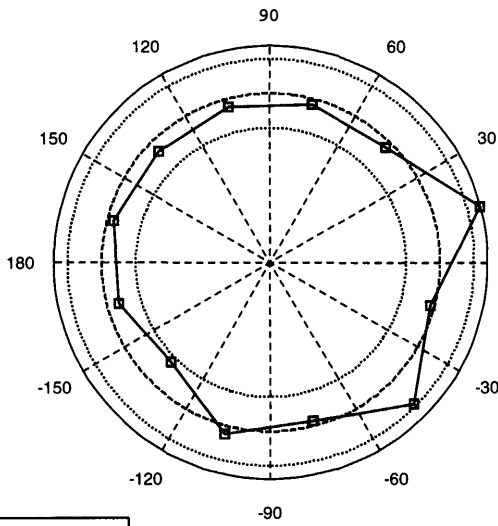$$Z_{i,j} = \left(Z_i\sqrt{N_j} - Z_j\sqrt{N_i}\right)/\sqrt{N_i + N_j}$$

which separates the females from all operators at the level $Z_{F,A} = .976$ ($p = .165$); the females from the males at $Z_{F,M} = 2.108$ ($p = .018$); and the groups from all operators at $Z_{G,A} = 1.470$ (p $= .071$).

In other experimental contexts[9] we have found it useful to define a "prolific operator" subset of participants, *i.e.* those whose extended commitment to the generation of data allows more incisive identification of individual performance characteristics, and essentially obviates any "optional stopping" confounds.[10] For this experiment, generation of five or more sets was established as the threshold criterion for the category, and the summary results for those prolific operators are shown in reference 7. The statistical yield of this dataset has been weakened somewhat by the exclusion of two significant female operators who performed only four sets each, and by its somewhat smaller overall size, but otherwise it closely resembles the full data array, and henceforth will not be pursued separately.

The same body of all-operator data may be subjected to a more detailed examination of the exit-angle distributions, with the results displayed in the polar plots of Figures 4–8. For this analysis we have divided the 360° azimuth of the robot platform into 12 sectors and plotted therein as radial excursions the lumped experimental populations of those exit angles for the 0° and 180° intentional efforts, superimposed on the mean value and the two-tailed 95% inner- and outer-bound confidence limit circles. Figure 4, which presents a direct comparison of the 0" and 180° efforts, shows a clear bias of both datasets toward the 0" hemicircle, which is confirmed by the attached statistical calculations (detailed in reference 7), and is probably indicative of some mechanical asymmetry in the initial alignment of the device or its platform. This suspicion is supported by similar patterns in the relevant calibration data (Figure 5). We should concentrate, therefore, on the accumulated population differences between the intentional data and the calibrations (Figure 6), or between the 0" and 180" populations around the twelve sectors (Figure 7), where such artifactual biases should cancel out. In neither of these formats do we see a statistically significant 0"–180" difference in the all-operator data, although clear distinctions between the female and male data are evident in Figure 8.

Key to Figures 4–8:

Z_p: Z-scores of empirical exit-angle bin population projections on the 0°–180° axis (*cf.* Appendix B-2 of reference 7).

p_Z: chance probability of Z_p.

χ^2:   chi-squared calculations over empirical bin population 2-scores, *i.e.* $\sum_{bins} Z_p^2$, to be compared with the number of degrees of freedom (number of bins minus one) to estimate the structural probabilities of the Z distributions, compared to chance expectations.

p_χ: chance probabilities of χ^2 values.

$\chi^2_{0,180}$:   goodness-of-fit chi-squared calculations comparing 0° and 180° distributions (*cf.* Appendix B-3 of reference 7).

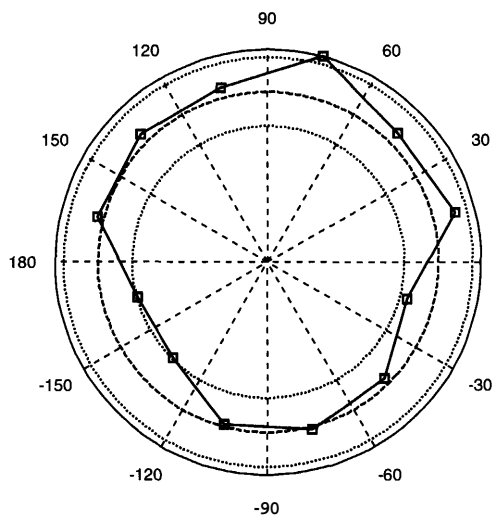χ^2_{fm}:   same comparison of female and male datasets.

a) $\underline{0°}$

$Z_p = 1.807$
$p_z = .031$
$\chi^2 = 8.132$
$p_\chi = .701$

empirical bin populations
expected populations
two-tailed 95% inner
and outer confidence limits

$\chi^2_{0,180} = 10.63$

$p_\chi = .475$

b) $\underline{180°}$

$Z_p = 1.026$
$p_z = .152$
$\chi^2 = 9.340$
$p_\chi = .591$

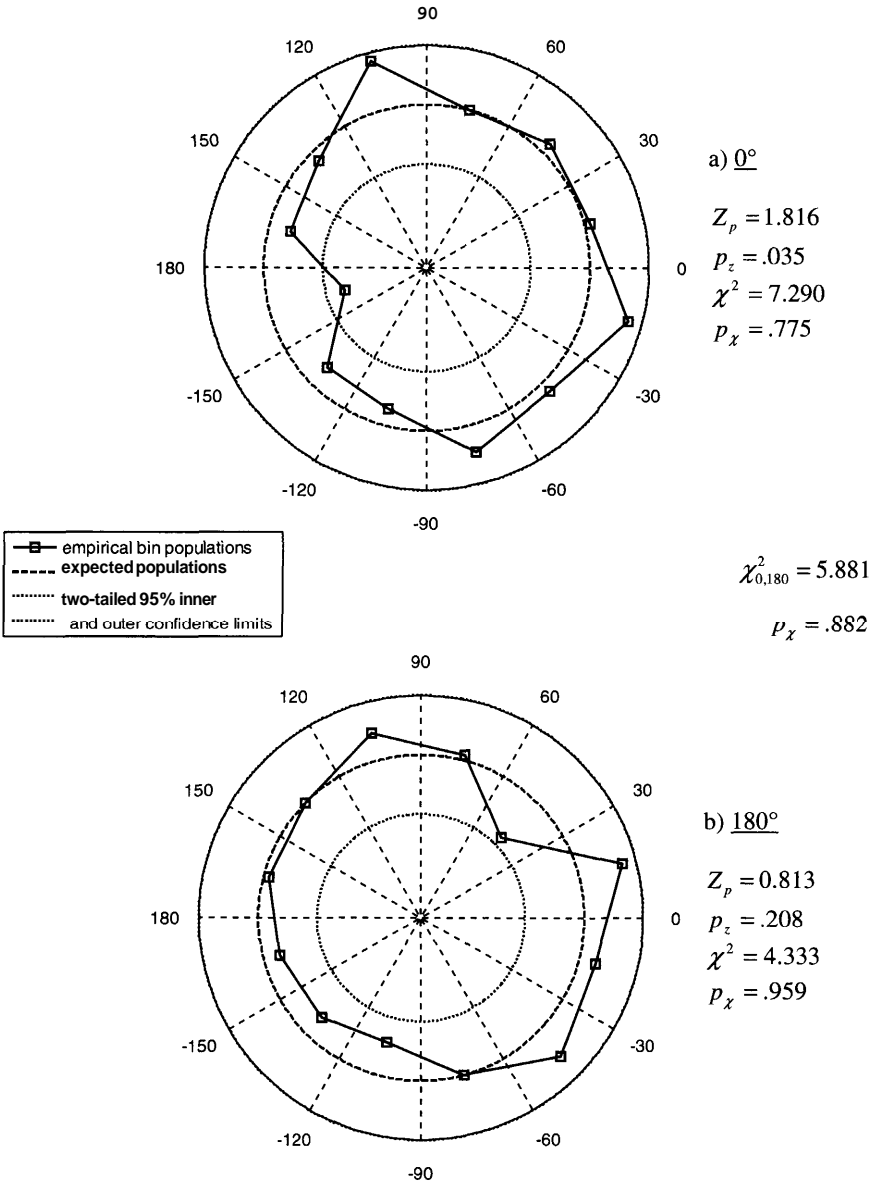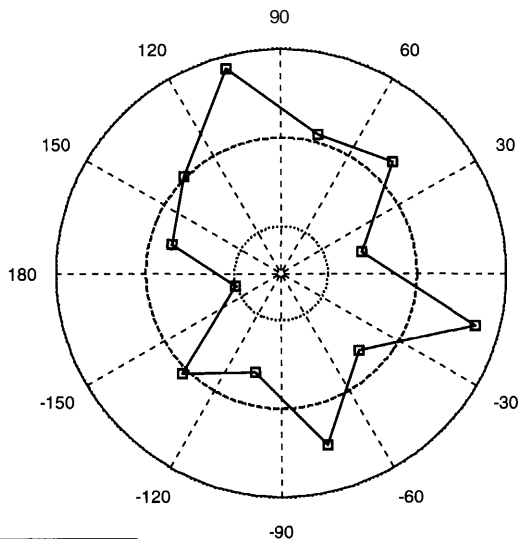Fig. 4. a, b. Azimuthal distributions for 0" and 180" intentions: All operators, 1103 paired runs each.

Fig. 5. a, b. Azimuthal distributions for 0° and 180" intentions: All relevant calibrations, split into artificial run pairs.
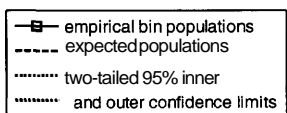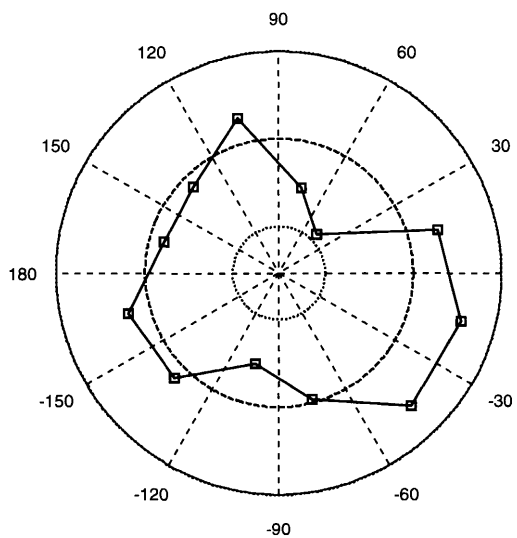
a) $\underline{0°}$

$Z_p = 1.016$

$p_z = .155$

$\chi^2 = 11.751$

$p_\chi = .383$

- empirical bin populations
- expected populations
- two-tailed 95% inner
- and outer confidence limits

$\chi^2_{0,180} = 10.7013$

$p_\chi = .4686$

b) $\underline{180°}$

$Z_p = 0.412$

$p_z = .340$

$\chi^2 = 8.103$

$p_\chi = .704$

Fig. **6.** a, b. Azimuthal distributions for 0" and 180° intentions subtracted from calibration data: All operators.
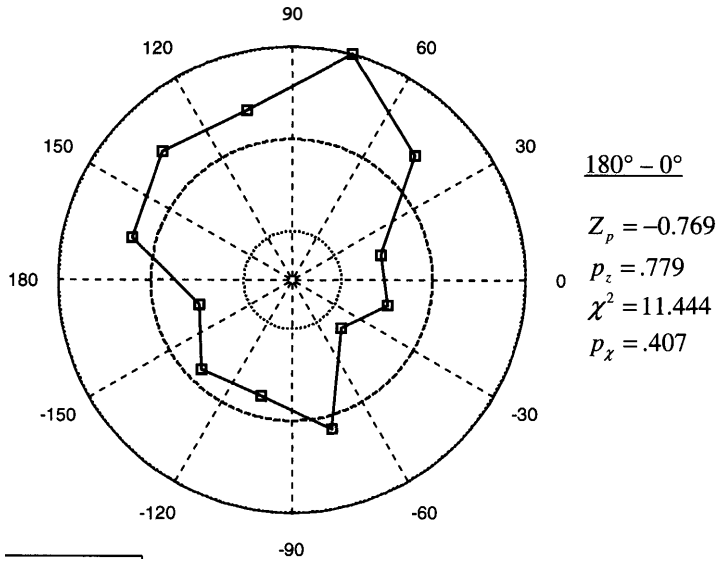
$$\underline{180° - 0°}$$

$$Z_p = -0.769$$
$$p_z = .779$$
$$\chi^2 = 11.444$$
$$p_\chi = .407$$

Fig. 7. Differences in azimuthal populations of 180° and 0" intention data: All operators.

Perhaps most indicative are direct differential comparisons of the 0" and 180" data obtained in the individual paired experimental sets, as shown in Figures 9–16. (The "cardioid" shapes of these polar graphs devolve from the use of the angle dzfferences as the azimuthal coordinate, wherein for chance data, full 180° separations are only rarely achievable, while 0° separations are obtainable from many more data combinations; *cf.* Appendix B-4 of reference 7.) To be noted are the close agreement of the polar segment difference distributions between all-data experiment and theory (Figure 9), experiment and calibration (Figure 10), and calibration and theory (Figure 11), compared to the more palpable separations of the female and male data patterns from calibrations (Figures 12 and 13), from theory (Figures 14 and 15), and from each other (Figure 16). Although the "goodness-of-fit" statistical calculations superimposed on the figures suggest no significant differences between the 0" and 180" data distributions, some distinctions between the female and male distributions can be identified.

3. Duration Experiments

An alternative protocol to assess possible operator influence on the robot motion has also been invoked, *e.g.* efforts to induce the robot to execute longer
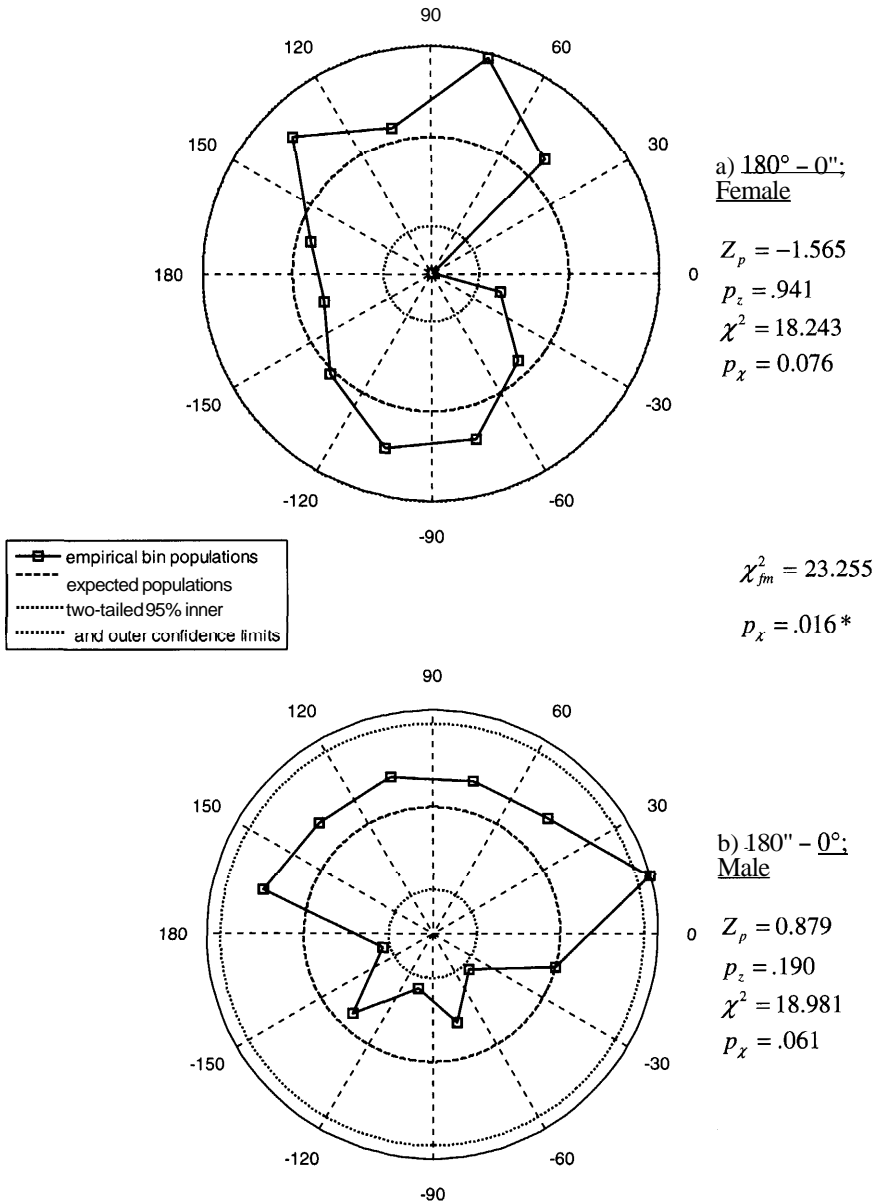
a) $\underline{180° - 0"}$;
Female

$Z_p = -1.565$

$p_z = .941$

$\chi^2 = 18.243$

$p_\chi = 0.076$

- ⊟— empirical bin populations
- --- expected populations
- ·········· two-tailed 95% inner
- ·········· and outer confidence limits

$\chi^2_{fm} = 23.255$

$p_\chi = .016*$

b) $\underline{180" - 0°}$;
Male

$Z_p = 0.879$

$p_z = .190$

$\chi^2 = 18.981$

$p_\chi = .061$

Fig. 8. Differences in azimuthal populations of 180" and 0" intention data: a) Female; b) Male.

or shorter trajectories before reaching the edge of the platform (time-of-flight) or equivalently, to cover longer or shorter total distances. (These could differ slightly because of the respective ratios of translation increments to rotation increments in the various datasets, or variations in the robot's translation and
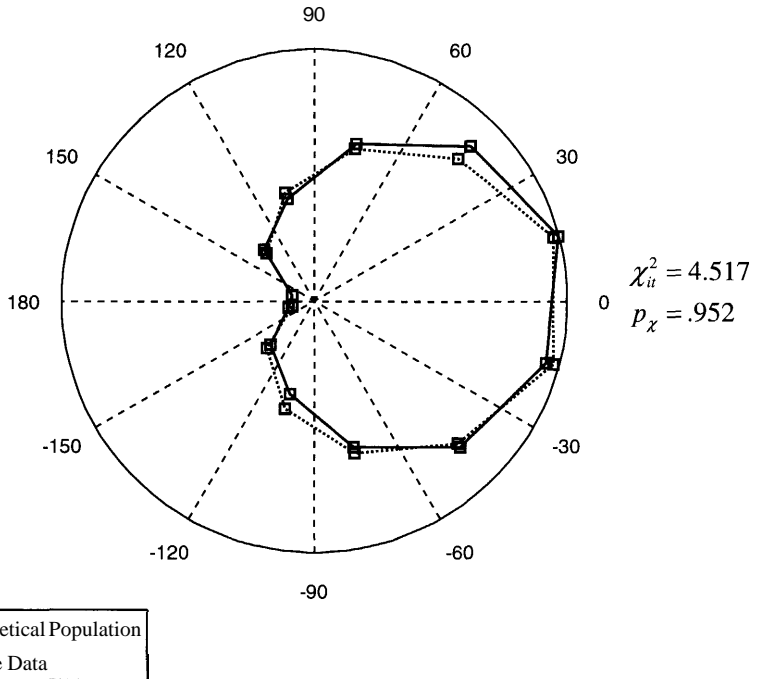
R. G. Jahn et al.

$$\chi^2_{it} = 4.517$$
$$p_\chi = .952$$

Fig. 9. Distributions of angular population differences between 180° and 0" intentions compared with theoretical chance expectations: 83 operators, 1103 paired sets.
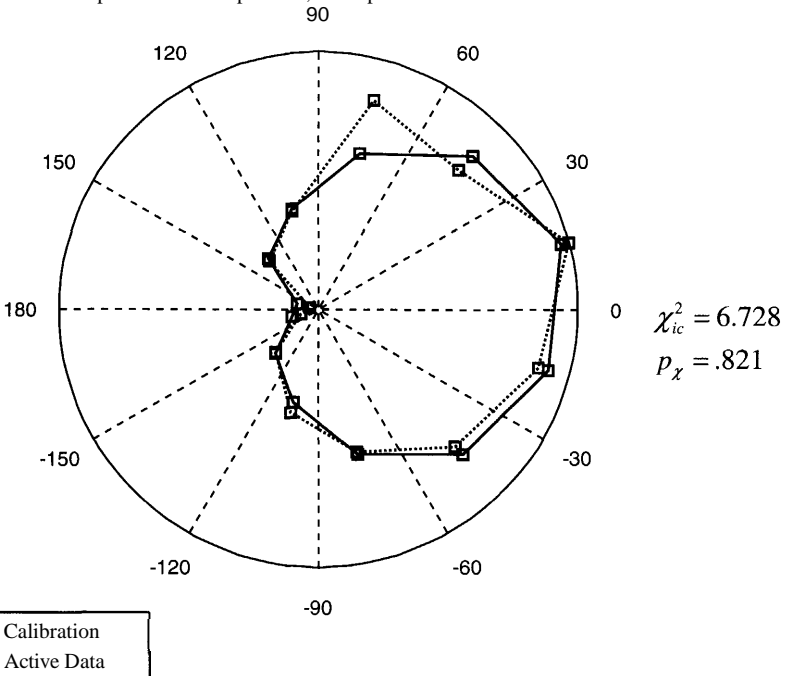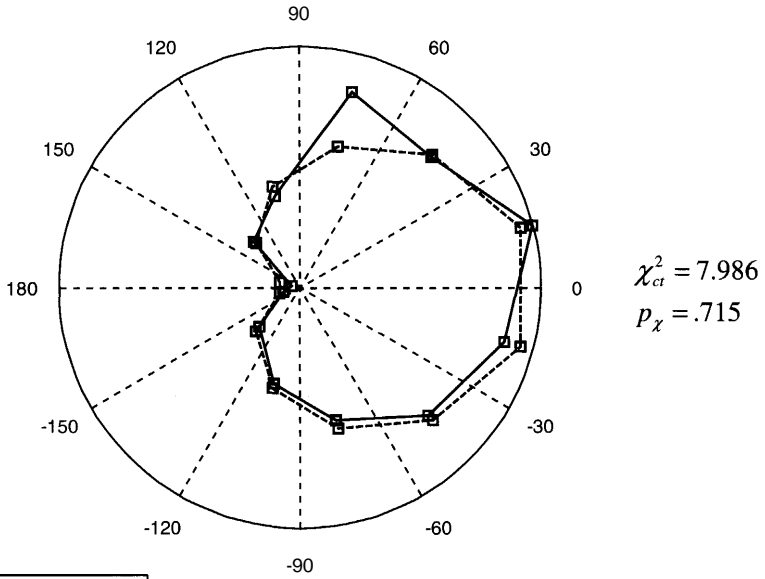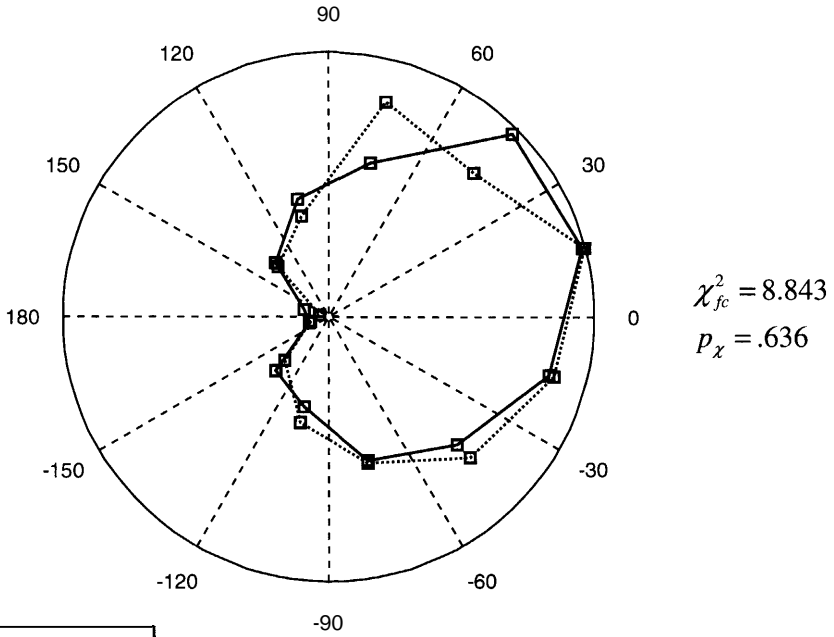

$$\chi^2_{ic} = 6.728$$
$$p_\chi = .821$$

Fig. 10. Distributions of angular population differences between 180" and 0" intentions compared with calibration data: 83 operators, 1103 paired sets, 353 calibration sets.

$$\chi^2_{ct} = 7.986$$
$$p_\chi = .715$$

Fig. 11. Distributions of angular population differences between 180" and 0": 353 calibrations compared with theoretical chance expectations.

$$\chi^2_{fc} = 8.843$$
$$p_\chi = .636$$

Fig. 12. Distributions of angular population differences between 180° and 0" intentions: 549 female datasets compared with 353 calibrations.

R. G. Jahn et **al.**

$$\chi_{mc}^2 = 7.553$$
$$p_\chi = .753$$

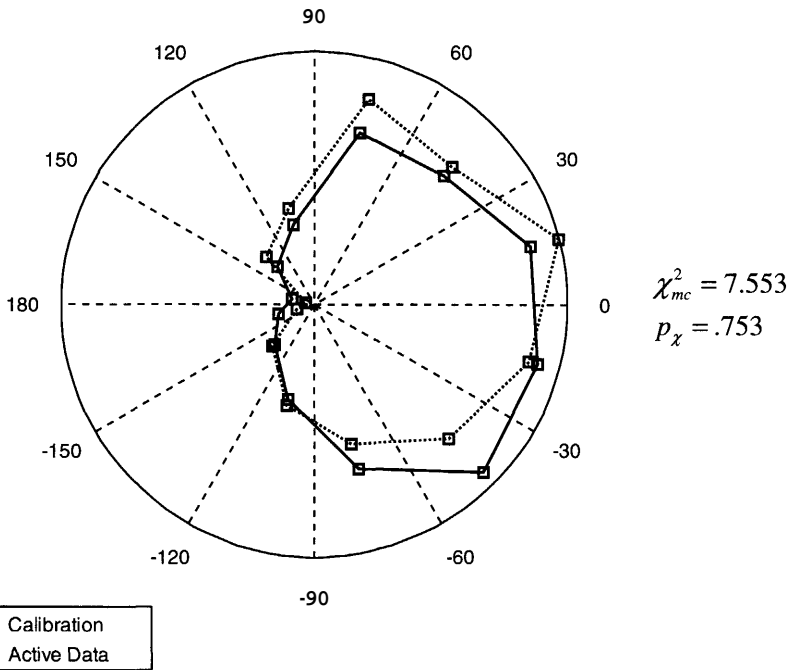Fig. 13. Distributions of angular population differences between 180° and 0" intentions: 416 male datasets compared with 353 calibrations.
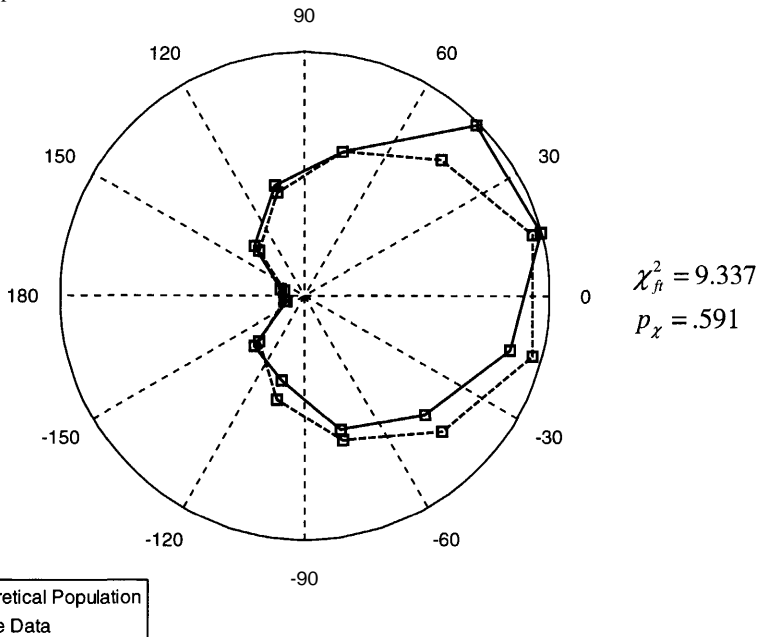

$$\chi_{ft}^2 = 9.337$$
$$p_\chi = .591$$

Fig. 14. Distributions of angular population differences between 180° and 0" intentions: 549 female datasets compared with theoretical chance expectations.
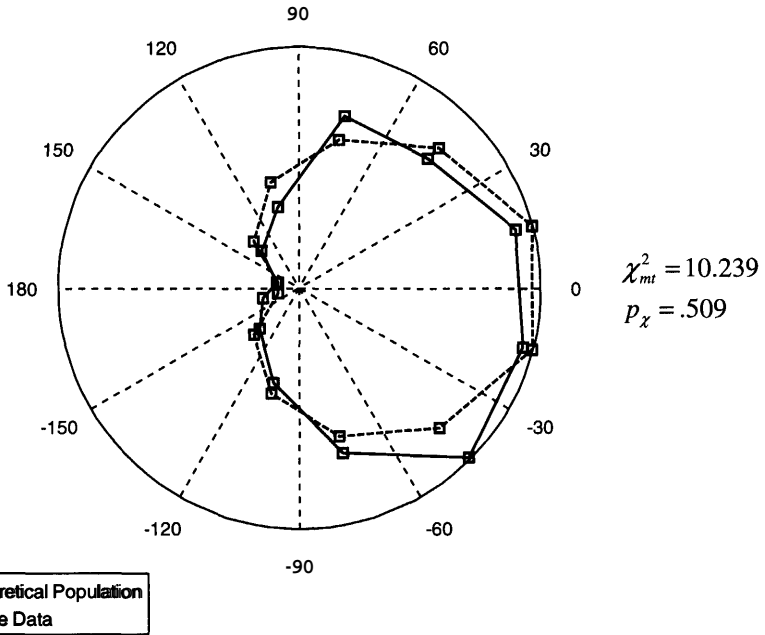
Fig. 15. Distributions of angular population differences between 180° and 0° intentions: 416 male datasets compared with chance expectations.
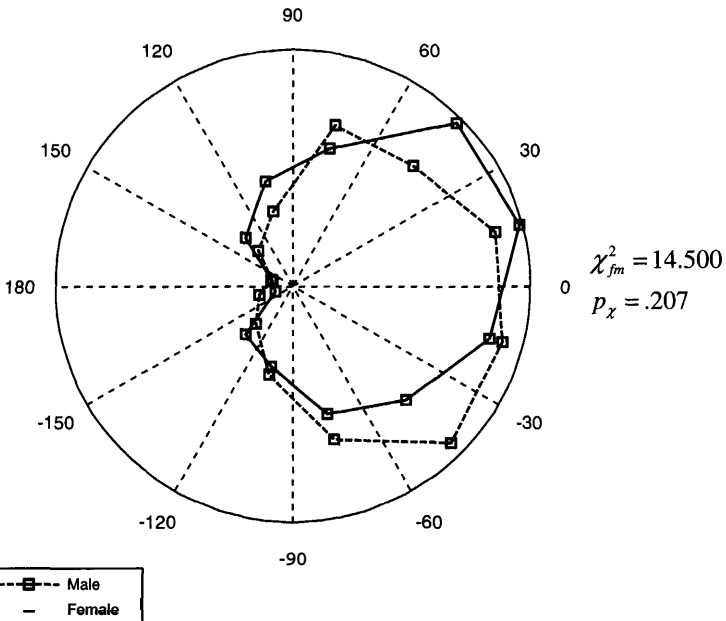

Fig. 16. Distributions of angular population differences between 180° and 0" intentions: 562 female datasets compared with 403 male datasets.

TABLE 2
Summary of All Time-of-Flight Data

Oper	# Ops	# Sets	$Z(p_z)$	ε	$\chi^2_{op}(p_\chi)$	# Oper +
All	33	678	1.085(.139)	.0417	23.687(.883)	18
Female	10	219	.978(.164)	.0661	12.245(.269)	4
Male	23	459	.669(.252)	.0312	11.442(.978)	15
Calibration	—	295	−.986(.838)	−.0574	—	—

Key

Ops: Number of individual operators, operator pairs, or groups contributing to databases.
Sets: Number of 0°, 180° paired sets performed.
Z: Equivalent statistical 2-scores computed from T-scores via Rosenthal approximation (*cf.* Appendix B of reference 7).
p_z: One-tailed probabilities of 2-scores against chance expectations.
E: Equivalent effect size, computed as $Z/\sqrt{\#Sets}$.
χ^2_{op}: Statistical chi-squared calculations over individual operator 2-scores; *i.e.* $\sum_{ops} Z^2$ to be compared with the number of degrees of freedom (number of operators) to estimate the structural probabilities of the Z distributions against chance expectations.
p_χ: chance probabilities of χ^2 values.
Oper +: Number of operators exceeding chance mean expectations.

rotation speeds due to battery run-down or wheel slippage.) The experimental results of the time-of-flight version are summarized in Table 2 and detailed in Appendix C of reference 7, again broken into all-operator, female, and male subgroups. (No Co-operator or Group Data were obtained under this protocol, and since only one operator failed to meet the prolific criterion, this distinction has been ignored.)

A few minor structural differences may be noted between the exit-angle data shown in Table 1 and these time-of-flight results. In the former, the overall opposite-to-intention male performance counteracted somewhat the female results of positive significance, reducing the "all" results below chance. Here, the male data show comparable performance to the female, but neither are sufficiently strong to drive the all-data results beyond chance. Of the 18 operators who achieved in the intended direction only one (female) produced an independently noteworthy result ($p = .0043$), and the χ^2_{op} values remain unremarkable. The effect sizes, again computed as $Z/\sqrt{\#Sets}$, are comparable with those of the exit-angle protocol, and with those of our "benchmark" experiments. [It perhaps should be noted that the smaller fraction of female contribution to this protocol version necessarily biases the gender comparison, *e.g.* if the female effect size were to be extrapolated over the male dataset size, the corresponding Z-score would be 1.483 ($p = .069$), and the combined Z-score would be 1.522 ($p = .064$).]

The data for the total distance variant of the duration experiments were extracted *ex post facto* from the same body of results just described. That is, the corresponding path lengths were computed from the camera traces of the same trajectories as a secondary empirical product of the data acquired under operator intentions to induce longer (or shorter) resident times of the robot on the

TABLE 3
Summary of All Trajectory Length Analyses

Oper	# Ops	# Sets	$Z(p_z)$	ε	$\chi^2_{op}(p_\chi)$	# Oper **+**
All	33	678	1.140(.**127**)	.0438	24.471(.858)	18
Female	10	219	1.001(.158)	.0676	12.736(.239)	4
Male	23	459	.721(.235)	.0337	11.734(.974)	14
Calibration	—	295	−.991(.839)	−.0577	—	—

Key: Same as Table 2

platform. As can be seen from Table 3, these results correspond closely to the time-of-flight measures both in structure and overall effect size, thereby reassuring us regarding the integrity of the robot motion and allowing us to combine them for subsequent interpretations.

4. Discussion

In several respects, the empirical results of these robot experiments are consistent with those of a number of other human/machine interaction studies performed in this laboratory over its many years of operation, using a wide range of physical systems as targets for the intentions of large numbers of uncompensated, volunteer operators. More specifically, here we again have found:

1) Marginally significant overall anomalous correlations of machine performance with pre-stated operator intentions;
2) Excessive fractions of individual operator achievements beyond chance expectation;
3) Disparities in performance between female and male operators;
4) Few, if any, "superstar" performances;
5) Idiosyncratic operator sensitivities to protocol and feedback modalities;
6) Other departures of structural aspects of the data from chance expectations, most notably the outlying performance of the small number of operator groups.

The last feature may merit some passing comments with respect to the desirability of attempting to replicate this group effectiveness in this, and other, experimental contexts. Given the logistical problems of convening groups of dedicated operators for more than one experimental session, the number of sets acquired for the exit-angle studies was statistically small, and none were obtained for either of the duration protocols. (A similar dearth of group data prevails for our many other human/machine experiments, leaving little basis for comparison or generalization.) Confounding the robot situation, yet worthy of note in its own right, was the fact that several of the groups comprised children around ten years of age, whose evident spontaneous enthusiasm for participation may have been a salient factor in their performance. While there has been

considerable parapsychological attention to group effects in other contexts, *e.g.*
healing, séances, mediumship, and apparitions, etc., more extensive studies of
the importance of this factor in controlled physical experimentation seem justified.

With this exception, the reappearance in the robot data patterns of the
characteristics just listed does not so much provide major new insights, as it
underscores the fundamental character of the phenomena--elusive, irreplicable,
and subjectively correlated as they may be. As such, these studies take a useful
supporting position in our ongoing efforts to formulate generic specifications of
all forms of consciousness-related anomalous physical phenomena.

5. Implications, Applications, Speculations

From its inception, the PEAR program has pursued its studies of anomalous
phenomena from the perspectives, and to the purposes, of the applied physical
sciences. This has entailed the empirical and theoretical acquisition of
fundamental understanding at both the epistemological and ontological levels,
as well as consideration of the implications and applications thereof for
pragmatic purposes within contemporary and future technologies. The latter
necessarily entails both negative and positive aspects. On the one hand,
legitimate concerns arise regarding the integrity of delicately poised information
processing devices and systems, particularly those that embody a random
component, functioning in emotional proximity to human operators. On the
other hand, speculations can be made regarding possibilities for beneficial
practical applications of the insights and technologies that might ultimately be
derived from the basic research efforts.'

In the particular context of the anomalous human/robot interactions reported
here, it might seem that such an erratic device as this whimsical roving vehicle
would have little potential for practical deployment beyond a children's toy or an
adult coffee-table curiosity, wherein its consciousness-correlated aberrations
would be of no major consequence. But in fact, we are well into a cultural age
where robotic technology is becoming widely utilized to perform many services
to relieve human operators of various tedious, difficult, or dangerous functions.
Robotic vacuum cleaners and lawn sprinklers already can be ordered on-line;
robotic equipment is routinely deployed for surveillance and service in hostile
radioactive and heavy manufacturing environments; and commitment of certain
medical diagnostics and treatment to miniaturized robotic devices is now being
seriously considered and in some cases utilized. In this latter context
particularly, and many others as well, the escalating advances in the micro-
and nano-sciences and technologies presage an era of miniaturized mobile
devices that will navigate microscopic terrains, including our physiological
systems, providing information and interventions that could be achieved in no
other way. Even at this primitive stage, protection from inadvertent or malicious
mis-applications of any such futuristic equipment should be borne in mind,
along with their potential consciousness-coupled enhancements.

While our basic research to date has enabled us to outline certain charac-
teristics of situations wherein anomalous mind/machine interactions may arise,''
we are clearly a long way from reliable invocation of consciousness-mediated
control of even such rudimentary vehicles as that employed in the experiments
reported here, let alone of their much more sophisticated siblings and descen-
dants. Nevertheless, the history of biofeedback successes, the proliferation of
robotic technologies, and the recent reports of physical control systems
responsive to operator attitudes[12] suggest that further fundamental study of this
form of mind/machine interaction may well be worthwhile. Certainly the distant
vision of the ingestion or insertion of dedicated micro- or nano-robotic devices
that could be willed preferentially to perform particular diagnostic or therapeutic
functions within our biological frameworks, or any other accessible complex
systems, should not be categorically dismissed.

Acknowledgments

References

1. Jahn, R. G., & Dunne, B. J. (2005). The PEAR Proposition. *Journal of Scientific Exploration, 19,*
    195–246.
2. Janin, P. (1986). The tychoscope. *Journal of the Society for Psychical Research, 53,* 341.
3. Tanguy, R. (1987). *Un Réseau de Mobiles Autonomes pour L'Apprentissage de la Communication.*
    Doctoral thesis, Université Paris 6, 2 décembre 1987.
4. Péoc'h, R. (1988). Chicken imprinting and the tychoscope: An Anpsi experiment. *Journal of the
    Society for Psychical Research, 55,* 1.
5. Péoc'h, R. (1995). Psychokinetic action of young chicks on the path of an illuminated source.
    Journal of Scientific Exploration, 9, 223–229.

6. Nelson, R. G. (1996). Report on Gate Pilot Protocol for Robot. PEAR Internal White Paper.
7. Jahn, R. G., Dunne, B. J., Acunzo, D. J., & Hoeger, E. S. (2006). *Response of an REG-driven robot to operator intention.* Technical Note PEAR 2006.03, November. Princeton NJ: Princeton University.
8. Jahn, R. G., Dunne, B. J., Nelson, R. D., Dobyns, Y. H., & Bradish, G. J. (1997). Correlations of random binary sequences with pre-stated operator intention: A review of a 12-year program. *Journal of Scientific Exploration, 11,* 345–367.
9. Dunne, B. J., Dobyns, Y. H., Jahn, R. G., & Nelson, R. D. (1994). Series position effects in random event generator experiments, *with an Appendix,* serial position effects in the psychological literature, by Thompson, **A.** *Journal of Scientific Exploration, 8,* 197–215.
10. Dobyns, Y. (2006). Personal communication.
11. Jahn, R. G., & Dunne, B. J. (2004). Sensors, filters, and the source of reality. *Journal of Scientific Exploration, 18,* 547–570.
12. Klouzal, T. J., & Plotke, R. J. (2006). Personal communication.

Appendix: Experimental Equipment

The robot assembly includes a two-wheeled mobile vehicle with nose- and tail-drags, a circular table on which it may move freely, and an optical detection and data recording system. The outer shell of the robot is a half-sphere of radius 15 cm that encloses a chassis supporting a dedicated power supply and a microelectronic REG. The device is propelled by two independent battery-powered electric clock motors, each connected to one of the robot's wheels. The motion is a succession of alternating rotations and translations for which the angles and lengths are determined randomly by the internal REG, whose processor generates random numbers by summing its output bites. The theoretical expected sum is subtracted from these numbers to obtain random digits that have null mean values. These are presented as 5-Hz successions of "tics," whose period defines a time unit for the behavior of the robot.

Once switched on, the robot motion begins with a rotation, after which it alternates forward translations with subsequent rotations. When the robot is due to start a translation, the system compares the last generated random number with two values that separate the theoretical distribution into three equal segments, on the basis of which it goes forward for 4, 5, or 6 tics, with equal probability. After completing the translation, the robot determines whether to rotate clockwise or counter-clockwise, based upon whether the next value generated is positive or negative. If the value is null, the robot makes no rotation, but proceeds through another translation, for which the distance is computed at the following tic. In its rotation mode, the robot examines every number generated during the consecutive tics in order to determine whether to continue its rotation or to stop. The threshold is designed to have a probability of approximately 0.1 to stop at each successive tic.

On top of the "dome", on the axis of rotation, an LED is installed that allows an overhead digital camera to detect and record the motion of the robot. The x and y coordinates of this LED position are recorded three times per second, along with the time of measurement. These files are the basis for all subsequent analyses of the robot trajectories.